Available online at www.sciencedirect.com
SCIENCE DIRECT®
PERGAMON
Polyhedron 22 (2003) 1981–1987
POLYHEDRON
www.elsevier.com/locate/poly

Hyperfine coupling of the cyanide ions and crystal water molecules of three dimensional magnetic polycyanides as studied by solid-state ^{13}C- and ^{2}H NMR

Hiroki Ishiyama, Goro Maruta, Taichi Kobayashi, Sadamu Takeda *

Division of Chemistry, Graduate School of Science, Hokkaido University, Sapporo 060-0810, Japan

Received 6 October 2002; accepted 19 December 2002

Abstract

The hyperfine coupling constant (HFCC) of a CN ligand must be sensitive to its coordination bond and local magnetic structures in three dimensional magnetic polycyanide such as Prussian-blue analogs. The local magnetic structure of $Rb_{0.90}Mn_{1.05}[Fe(^{13}CN)_6]\cdot 3H_2O$, which exhibits a thermally induced spin phase transition near room temperature with a wide hysteresis, was investigated in the high and low spin phase by solid-state ^{13}C NMR spectrum of the ^{13}CN ligand. Major and minor peaks were observed in the high spin phase $Fe^{III}(S=1/2)$–^{13}CN–$Mn^{II}(S=5/2)$, while the major and two other peaks were observed in the low spin phase. These results indicate a slightly non-uniform structure of $Rb_{0.90}Mn_{1.05}[Fe(^{13}CN)_6]\cdot 3H_2O$. The HFCC of a carbon atom was estimated from the slope of the ^{13}C NMR shift as a function of inverse temperature. The HFCC of the Fe–^{13}CN–Mn of $Rb_{0.90}Mn_{1.05}[Fe(^{13}CN)_6]\cdot 3H_2O$ is positive in both spin phases, while that of the $Fe^{III}(S=1/2)$–^{13}CN of $(Na_{0.4}K_{0.6})_3[Fe^{III}(S=1/2)(^{13}CN)_6]$ is negative. This result indicates that the effect of the spin of Mn ion exceeds the negative contribution of Fe ion in the Fe–CN–Mn system. On the other hand, the HFCC is negative for $Na_{0.5}Co_{1.26}[Fe(^{13}CN)_6]\cdot n H_2O$ in the high spin phase, where the spin of $Fe^{III}(S=1/2)$ ion dominates the HFCC in the $Fe^{III}(S=1/2)$–CN–$Co^{II}(S=3/2)$ system. The positive and negative contributions from $Mn^{II}(S=5/2)$ and $Cr^{III}(S=3/2)$, respectively, dominate the ^{13}C NMR shift in different temperature regions in the $Cr^{III}(S=3/2)$–^{13}CN–$Mn^{II}(S=5/2)$ system of $Mn^{II}_{1.5}[Cr^{III}(^{13}CN)_6]\cdot n H_2O$.

Keywords: Prussian-blue analogs; Local magnetic structures; Solid-state ^{13}C NMR; Hyperfine coupling of CN ions; Solid-state high-resolution deuterium NMR; Crystal water molecules

1. Introduction

Transition metal polycyanides show interesting phenomena such as, for example, photomagnetism [1,2], a magnet exhibiting magnetic pole inversion [3], and spin transitions accompanied with electron transfer [4,5]. These interesting properties are based on a combination of magnetic metal ions, doped non-magnetic ions to control the strength of the ligand field of the magnetic ions [5], and a cyanide (CN) ion as a three dimensional magnetic coupler. The hyperfine coupling constant (HFCC) of a CN ligand must be sensitive to its coordination bond and local magnetic structures of the three dimensional polycyanide such as the Prussian-blue analogs depicted in Fig. 1.

In recent years, Ohkoshi et al. [6] reported that the magnetic polycyanide $RbMn[Fe(CN)_6]$ undergoes a spin phase transition with a wide hysteresis near room temperature. To elucidate the local magnetic structures of this system, we measured the solid-state ^{13}C NMR spectrum in the high and low spin phases. The HFCC of the Fe–^{13}CN–Mn system was estimated from the temperature dependence of the ^{13}C NMR shift and was compared with those of the Fe–^{13}CN–Co and Cr–^{13}CN–Mn systems of Prussian-blue analogs to see a difference of electron spin induction on the CN ions among various combinations of two magnetic ions M–^{13}CN–M′. The HFCC is useful for elucidating the

* Corresponding author. Tel.: +81-11-706-3505; fax: +81-11-706-4841.
E-mail address: stakeda@sci.hokudai.ac.jp (S. Takeda).

0277-5387/03/$ - see front matter
doi:10.1016/S0277-5387(03)00163-3

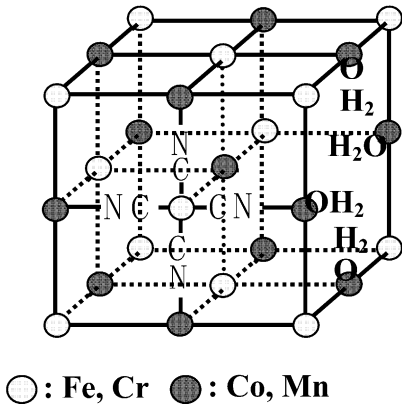

Fig. 1. Schematic view of M–CN–M′ polycyanide, Prussian-blue analog.

magnetic interaction between the magnetic metal ions through the CN ion.

The local environments of the crystal water molecules were also studied by magic angle spinning deuterium NMR (MAS D NMR) spectrum for $Na_{0.5}Co_{1.26}[Fe(CN)_6]\cdot nD_2O$ and $(Ni_xMn_{1-x})_{1.5}[Cr(CN)_6]\cdot nD_2O$. In the case of $Na_xCo_y[Fe(CN)_6]\cdot nH_2O$, the crystal water molecules control the ligand field of the cobalt ion, inducing a spin phase transition accompanied with an electron transfer [5]. $(Ni_xMn_{1-x})_{1.5}[Cr(CN)_6]\cdot nD_2O$ shows an inversion of magnetic pole due to the coexistence of ferromagnetic and antiferromagnetic exchange interactions [3].

2. Method and experiment

2.1. Solid-state NMR and magnetic susceptibility measurement

The ^{13}C NMR spectrum was measured by an echo pulse sequence for static powder crystalline sample at an external magnetic field of 7.05 T with a Bruker DSX300 spectrometer. Various irradiation frequencies were used to cover the wide spectrum. The envelope of all the echo signals displays a whole spectral line shape. Line shape fitting was carried out by considering the anisotropy of the dipole interaction between ^{13}C nucleus and electron spins of magnetic ions and a broadening factor and this gave an isotropic shift. The shift was measured from the powder crystalline sample of $K^{13}CN$ (169.6 ppm from TMS). Neglecting the zero field splitting, the observed isotropic shift δ_{iso} consists of the Fermi contact term, the dipole interaction term (pseudo contact) and the temperature independent diamagnetic term (chemical shift) as follows [7,8],

$$\delta_{iso} = \delta_{Fermi} + \delta_{Pseudo} + \delta_{dia} \quad (1)$$

$$\delta_{Fermi} + \delta_{Pseudo} = \frac{\mu_B}{3k_BT}\frac{A'_C}{\gamma_C/2\pi} \quad (2)$$

Electron spin induced on the ^{13}C nucleus by electron spins of magnetic metal ions causes a Fermi contact shift of the NMR resonance line, whereas anisotropy of the g-tensor of magnetic metal ions gives a pseudo-contact shift. The coefficient A'_C in Eq. (2) is defined as the HFCC of the ^{13}C nucleus in Hz unit, including the contributions from the two magnetic ions of M–^{13}CN–M′. The anisotropic g tensors terms and spin quantum numbers of the two magnetic ions are also included in A'_C. The present definition of the coefficient A'_C is not the usual one [7,8]. If we could measure the isotropic shift of the ^{13}C NMR spectrum in a very wide temperature region, two individual HFCC's due to each magnetic ion would separately be determined.

MAS D NMR spectra were measured by a similar method described in Ref. [9] at a resonance frequency of 46.1 MHz and at a magic angle spinning speed of approximately 10 kHz with a Bruker DSX300 spectrometer. The MAS technique gives an isotropic shift of deuterium. The thermometer of the MAS NMR probe and an effect of spinning speed on temperature increase were carefully calibrated [9,10]. The D NMR shift was measured from the external second reference of CD_3OD (CD_3: 3.35 ppm).

Direct current magnetic susceptibility was measured with SQUID magnetometer (Quantum Design MPMS 5) at an external magnetic field of 1 T.

2.2. Sample preparation

The ^{13}C enriched rubidium(I) manganese(II) hexacyanoferrate(III) was prepared by adding slowly an aqueous solution of 0.1 M $Mn^{II}Cl_2$ and 1 M $Rb^{I}Cl$ to an aqueous solution of 0.1M $(Na_{0.4}K_{0.6})_3[Fe^{III}(^{13}CN)_6]$ and 1 M $Rb^{I}Cl$ at room temperature to yield a brown precipitate. Elemental analyses for C, H and N and ICP-AES for metal ions showed the formula of $Rb^{I}_{0.90}Mn^{II}_{1.05}[Fe^{III}(^{13}CN)_6]\cdot 3H_2O$: Calc.(found): Rb, 18.9%(19.7); Mn, 14.2%(15.0); Fe, 13.7%(13.4); C, 19.2%(19.2); N, 20.7%(20.7); H, 1.5%(0.7). The ^{13}C enriched $(Na_{0.4}K_{0.6})_4[Fe^{II}(^{13}CN)_6]$ was synthesized from $K^{13}CN$ and $(NH_4)_2Fe^{II}(SO_4)_2$ under the basic condition with using NaOH and then $(Na_{0.4}K_{0.6})_4[Fe^{II}(^{13}CN)_6]$ was oxidized to yield $(Na_{0.4}K_{0.6})_3[Fe^{III}(^{13}CN)_6]$.

The ^{13}C enriched sodium(I) cobalt(II) hexacyanoferrate(III) was synthesized by adding an aqueous solution of 4 mM $Co^{II}Cl_2$ and 4 M $Na^{I}Cl$ to an aqueous solution of 4 mM $(Na_{0.4}K_{0.6})_3[Fe^{III}(^{13}CN)_6]$ and 4 M $Na^{I}Cl$. Elemental analyses (ICP-AES) of metal ions showed their contents, Na, 3.21%; Co, 18.8% and Fe, 14.1%. The relative amount of the metal ions indicated the formula of $Na_{0.5}Co_{1.26}[Fe(^{13}CN)_6]\cdot nH_2O$. The com-

pound with deuterated crystal water molecules was prepared similarly in D_2O solution by using anhydrous $Co^{II}Cl_2$ to ensure the complete deuteration of the crystal water.

The ^{13}C enriched $K_3[Cr^{III}(^{13}CN)_6]$ was synthesized from CrO_3 and $K^{13}CN$ [11]. Then three ^{13}C enriched compounds, $(Ni^{II}_xMn^{II}_{1-x})_{1.5}[Cr^{III}(^{13}CN)_6]\cdot nH_2O$ where $x = 0$, 0.4 and 1, were prepared by a similar method reported in Ref. [3]. A 7 cm^3 aqueous solution of total concentration of 0.02 M of $(NiCl_2)_x(MnCl_2)_{1-x}$ was added to a 1 cm^3 aqueous solution of 0.1 M $K_3[Cr^{III}(^{13}CN)_6]$, yielding a powder crystal. The fraction x was 0, 0.4 and 1. For the synthesis of deuterated compounds, $(Ni^{II}_xMn^{II}_{1-x})_{1.5}[Cr^{III}(CN)_6]\cdot nD_2O$ where the fraction x was also 0, 0.4 and 1, D_2O solutions were used instead of H_2O solutions. The powder X-ray diffraction of all samples coincided with the results reported in Ref. [3].

3. Results and discussion

3.1. Local magnetic structures of $Rb_{0.90}Mn_{1.05}[Fe(^{13}CN)_6]\cdot 3H_2O$

Fig. 2 shows the magnetic susceptibility ($\chi_M T$) of $Rb_{0.90}Mn_{1.05}[Fe(^{13}CN)_6]\cdot 3H_2O$ as a function of temperature. The spin transition showed a wide hysteresis between decreasing and increasing temperature. This behavior is very similar to that of $RbMn[Fe(CN)_6]$ reported in Ref. [6]. But the transition temperature is slightly lower and the $\chi_M T$ value in the low spin phase is significantly larger than that of $RbMn[Fe(CN)_6]$. This result is brought about by a small content of Rb ions. A similar behavior was also observed by Tokoro et al. [12]. The powder X-ray diffraction at room temperature showed a mixture of the high and low spin phases, where the former is a face-centered cubic structure with a lattice constant of 10.52 Å. The lattice constant of

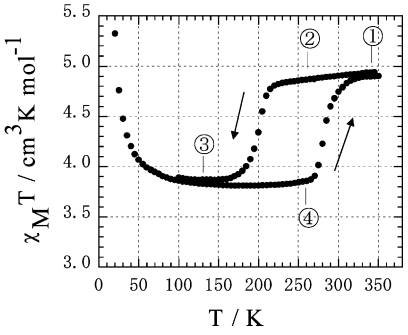

Fig. 2. Magnetic susceptibility $\chi_M T$ of $Rb_{0.90}Mn_{1.05}[Fe(^{13}CN)_6]\cdot 3H_2O$ as a function of temperature. The numbers ① through ④ in the figure indicate a relation between the magnetic susceptibility and the NMR spectrum shown in Fig. 3.

10.52 Å is the same as that reported for $RbMn[Fe(CN)_6]$ [6].

The temperature variation of the solid-state ^{13}C NMR spectrum of $Rb_{0.90}Mn_{1.05}[Fe(^{13}CN)_6]\cdot 3H_2O$ is depicted in Fig. 3. Typical spectra are shown in this figure. Each spectrum is composed of echo signals, where each echo signal was measured at different excitation frequencies to cover the wide spectrum. The envelope of all the echo signals shows the line shape of a powder spectrum. The spectrum was measured in a direction of decreasing temperature from 340 K down to 130 K and then in a direction of increasing temperature up to 293 K to follow the hysteresis of the spin phase transition. The spectra (a–c) are of the high spin phase, while the spectra (e–g) of the low spin phase. The spectra (d) and (h) show a pattern of a mixture of the high and low spin phases.

In the high spin phase, the fcc structure predicts only one ^{13}C NMR signal for CN ions. However, two signals were observed in this phase, suggesting a locally non-uniform structure of this material. An intense major signal appeared in the lower frequency region and a minor one in the higher frequency region. It is considered that the minor signal corresponds to the CN ions near a defect of $[Fe(CN)_6]$ ion or near an irregular position of the Rb ion in the interstitial site. Although the magnetic local structure is not completely uniform, the $\chi_M T$ value of 4.9 cm^3 K mol^{-1} in the high spin phase suggests the spin state of $Fe^{III}(S = 1/2)$–CN–$Mn^{II}(S = 5/2)$ [6]. The major signal apparently indicates an almost axial anisotropy of the dipole interaction between ^{13}C nucleus and electron spins of Fe and Mn ions. The line shape analysis of the major peak gave an isotropic NMR shift. The temperature variation of the isotropic shift is shown in Fig. 4 as a function of inverse temperature.

In the low spin phase, two signals in addition to the major peak were observed, as seen in Fig. 3(e–g). A non-uniform structure giving irregular g values of the magnetic ions or a non-uniform spin state was suggested by the present ^{13}C NMR spectrum for the low spin phase of $Rb_{0.90}Mn_{1.05}[Fe(^{13}CN)_6]\cdot 3H_2O$. The three components of the ^{13}C NMR spectrum may reflect the different magnetic local structures of the magnetic ions. Since all different local structures contribute to the bulk magnetic susceptibility, it seems difficult to determine concretely the spin state in the low spin phase from the magnetic susceptibility data shown in Fig. 2. The line width of the major signal in the low spin phase is remarkably small compared with that in the high spin phase, which is clearly seen by comparing the spectrum (c) for the high spin phase with the spectrum (g) for the low spin phase measured at the same temperature of 240 K. The line width reflects the spin state of the Fe and Mn ions, particularly the Mn ion. Since the line shape of the major peak in the low spin phase is almost

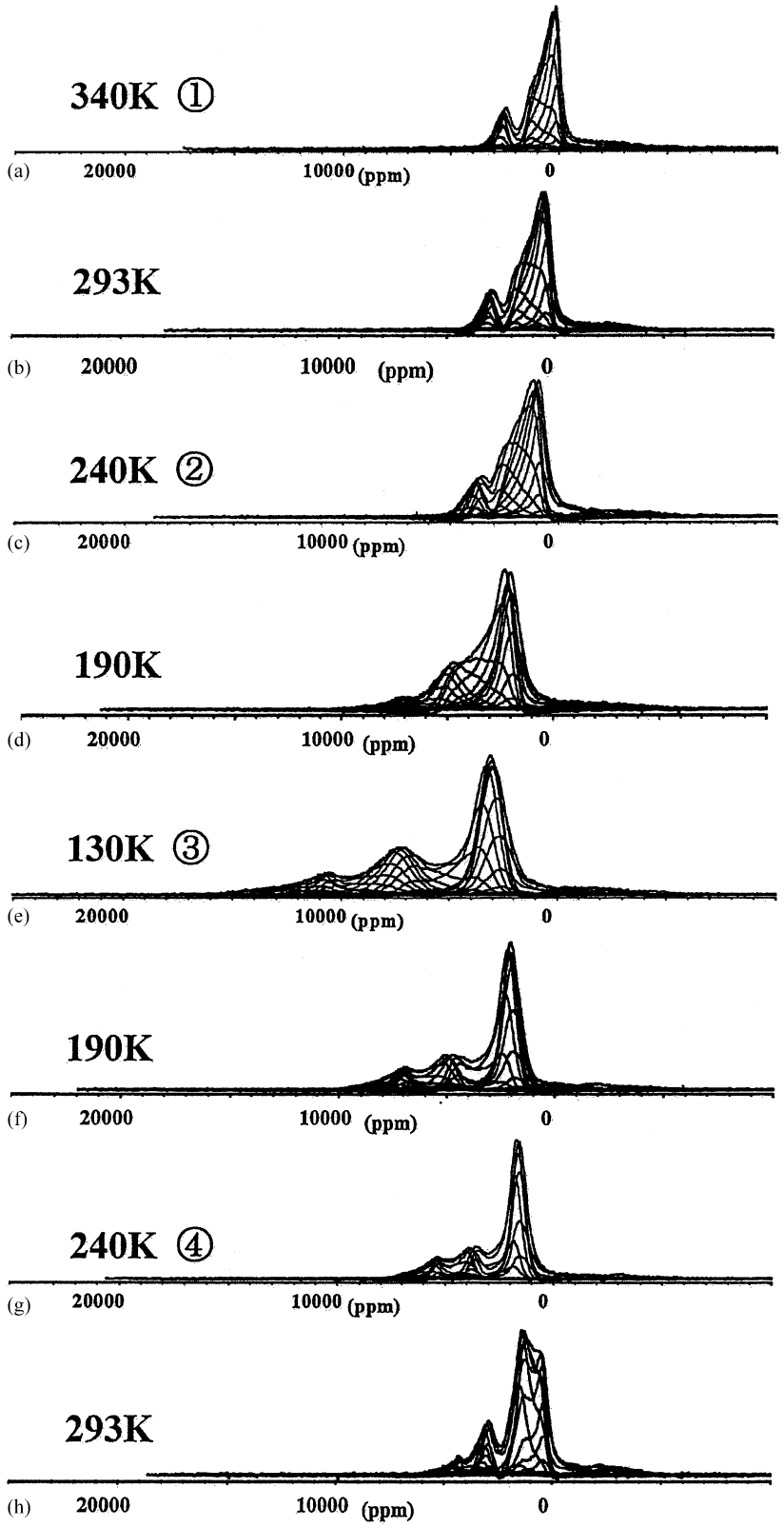

Fig. 3. Variation of the ^{13}C NMR spectrum of $Rb_{0.90}Mn_{1.05}[Fe(^{13}CN)_6]\cdot 3H_2O$. The spectrum was measured in a direction of decreasing temperature from 340 K down to 130 K and then in a direction of increasing temperature up to 293 K to follow the hysteresis of the spin phase transition. The spectra (a–c) are of the high spin phase, while the spectra (e–g) of the low spin phase. The spectra (d) and (h) show a pattern of a mixture of the high and low spin phases. The number shown after the temperature indicates a relation between the NMR spectrum and the magnetic susceptibility shown in Fig. 2.

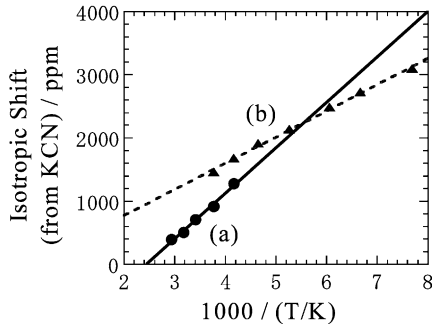

Fig. 4. Isotropic shift of ^{13}C NMR spectrum of $Rb_{0.90}Mn_{1.05}[Fe(^{13}CN)_6]\cdot 3H_2O$ as a function of inverse temperature. (a) high spin phase (●) and (b) low spin phase (▲).

symmetric and the anisotropy of the dipole interaction is not clear, the shift of the major peak in the low spin state was determined from the maximum point of the peak and was plotted as a function of inverse temperature in Fig. 4. The slope of the shift of the ^{13}C NMR spectrum is positive both for the high and low spin state of this Fe–^{13}CN–Mn system. This result indicates that the HFCC (A_C') in Eq. (2) is positive both for the high and low spin phases. The value of A_C' in Eq. (2) is +44 and +25 MHz for the high and the low spin phase.

3.2. Carbon hyperfine coupling of cyanide ions of various M–^{13}CN–M' systems

The temperature dependence of the shift of ^{13}C NMR spectrum of an isolated $[Fe^{III}(S=1/2)(^{13}CN)_6]^{3-}$ ion of $(Na_{0.4}K_{0.6})_3[Fe(^{13}CN)_6]$ is largely negative, i.e. $A_C' = -50$ MHz, as shown in Fig. 5 [13]. The carbon atom of the CN ion in this compound coordinates to the Fe ion and the nitrogen atom is free. Thus, the $Fe^{III}(S=1/2)$ ion induces a negative spin on the carbon atom of the CN ion. The negative spin on the carbon atom determined by polarized neutron diffraction experiment was reported for $Cs_2K[Fe^{III}(CN)_6]$ [14].

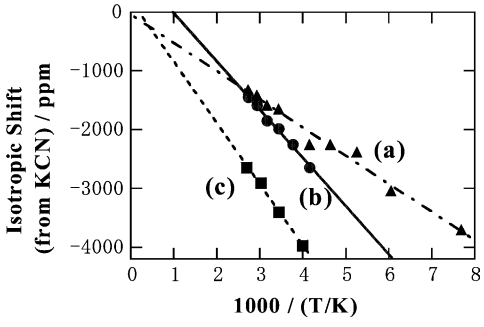

Fig. 5. Isotropic shift of ^{13}C NMR spectrum as a function of inverse temperature. (a) high spin state of $Li^{I}_{0.2}Co^{II}(S=3/2)_{1.40}[Fe^{III}(S=1/2)(^{13}CN)_6]\cdot nH_2O$, (▲) (b) high spin state of $Na^{I}_{0.5}Co^{II}(S=3/2)_{1.26}[Fe^{III}(S=1/2)(^{13}CN)_6]\cdot nH_2O$, (●) (c) $(Na^{I}_{0.4}K^{I}_{0.6})_3[Fe^{III}(S=1/2)(^{13}CN)_6]$ (■).

The Fe–CN–Co system $Na_{0.5}Co_{1.26}[Fe(^{13}CN)_6]\cdot nH_2O$ shows a spin transition around 240 K and the spin state of the high temperature phase is $Fe^{III}(S=1/2)$–^{13}CN–$Co^{II}(S=3/2)$. The similar compound $Li_{0.2}Co_{1.40}[Fe(^{13}CN)_6]\cdot nH_2O$ shows no apparent spin transition and the spin state is also $Fe^{III}(S=1/2)$–^{13}CN–$Co^{II}(S=3/2)$ [13]. The HFCC of the former and the latter compound in the high spin sate is $A_C' = -39$ and -23 MHz, respectively, which are smaller than $A_C' = -50$ MHz for the $Fe^{III}(S=1/2)$–^{13}CN of $(Na_{0.4}K_{0.6})_3[Fe(^{13}CN)_6]$. This result indicates that a negative contribution from $Fe^{III}(S=1/2)$ and a positive contribution from $Co^{II}(S=3/2)$ compete on the carbon atom of CN ion in the $Fe^{III}(S=1/2)$–^{13}CN–$Co^{II}(S=3/2)$ system and that the negative contribution from $Fe^{III}(S=1/2)$ exceeds the positive one from $Co^{II}(S=3/2)$ to dominate the HFCC in the temperature region displayed in Fig. 5.

On the contrary, the negative contribution from $Fe^{III}(S=1/2)$ is smaller than the positive one from $Mn^{II}(S=5/2)$ in the $Fe^{III}(S=1/2)$–^{13}CN–$Mn^{II}(S=5/2)$ system of $Rb_{0.90}Mn_{1.05}[Fe(^{13}CN)_6]\cdot 3H_2O$ in the temperature region shown in Fig. 4. Although the spin state of the low spin phase of this compound is not clearly determined at present, the positive contribution from the Mn ion exceeds the contribution from the Fe ion to exhibit the positive HFCC as seen from the positive slope of the ^{13}C NMR shift as a function of inverse temperature depicted in Fig. 4.

In the case of $Cr^{III}(S=3/2)$–^{13}CN–$Mn^{II}(S=5/2)$, each negative and positive contribution from the $Cr^{III}(S=3/2)$ and $Mn^{II}(S=5/2)$ ions, respectively, dominates the slope of ^{13}C NMR shift in the different temperature regions as described below. The isotropic ^{13}C NMR shift of $Mn^{II}(S=5/2)_{1.5}[Cr^{III}(S=3/2)(^{13}CN)_6]\cdot nH_2O$ is plotted in Fig. 6 as a function of inverse temperature, where the isotropic shift was determined by analyzing the anisotropic line shape of the powder sample as in the case of the high spin phase of $Rb_{0.90}Mn_{1.05}[Fe(^{13}CN)_6]\cdot 3H_2O$. The shift as a function of inverse temperature is not linear. It showed a minimum around 300 K. The negative contribution

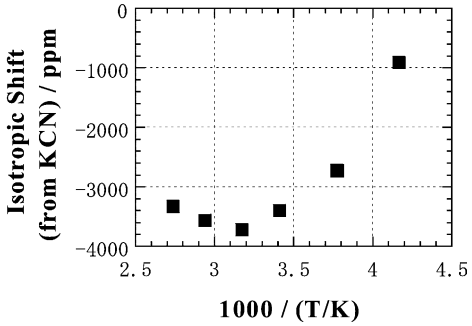

Fig. 6. Isotropic shift of ^{13}C NMR spectrum of $Mn^{II}(S=5/2)_{1.5}[Cr^{III}(S=3/2)(^{13}CN)_6]\cdot nH_2O$ as a function of inverse temperature.

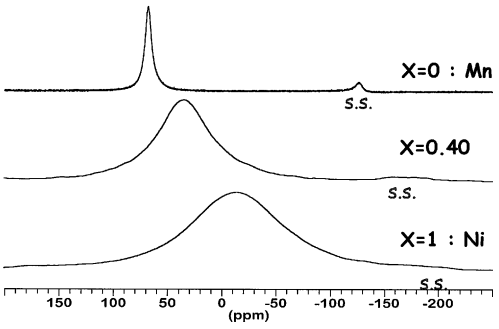

Fig. 7. MAS D NMR spectrum of $(Ni_x^{II}Mn_{1-x}^{II})_{1.5}[Cr^{III}(CN)_6]\cdot nD_2O$ measured at 9 kHz of spinning speed at 299 K. The fraction x is 0, 0.4 and 1. Spinning side bands are indicated by an abbreviation s.s.

from $Cr^{III}(S=3/2)$ dominates in the high temperature region, while the positive one from $Mn^{II}(S=5/2)$ in the low temperature region.

Each of the three systems, i.e. $Fe^{III}(S=1/2)$–^{13}CN–$Mn^{II}(S=5/2)$, $Fe^{III}(S=1/2)$–^{13}CN–$Co^{II}(S=3/2)$ and $Cr^{III}(S=3/2)$–^{13}CN–$Mn^{II}(S=5/2)$, exhibits a characteristic hyperfine coupling of the carbon atom of cyanide ion. This experimental result will be useful for the analysis of spin distribution and orbital interactions of these systems.

3.3. Character of crystal water molecules

For the $M_xCo_y[Fe(CN)_6]\cdot nH_2O$, the doping of alkali cation M is considered to control the ligand field of the cobalt ion by substituting the water molecule of $[Co(H_2O)_n(NC)_{6-n}]$ with cyanide ligands of $[Fe(CN)_6]$ to maintain the charge balance. The strength of the ligand field of the cobalt ion determines the spin state of Fe–CN–Co, i.e. high spin state $Fe^{III}(S=1/2)$–CN–$Co^{II}(S=3/2)$ or low spin state $Fe^{II}(S=0)$–CN–$Co^{III}(S=0)$ [5]. Thus, the character of the crystal water molecules is of interest and MAS D NMR spectrum of $Na_{0.5}Co_{1.26}[Fe(CN)_6]\cdot nD_2O$ was measured [13]. Three signals were identified at 2, −13 and −39 ppm at 364 K. The temperature variation of an envelope of all the spinning side bands of the MAS D NMR spectrum indicated that all D_2O molecules underwent a rapid overall rotation. This rotation became slow near 240 K as the temperature was decreased. However, a 180°-flip motion about the C_2-axis of the D_2O molecule remained rapid down to 200 K at least [13]. Therefore, the crystal water molecules are not rigidly bound to the cobalt ion in the temperature region of the spin phase transition of this compound.

Overall rotation of water molecules was also observed for $(Ni_x^{II}Mn_{1-x}^{II})_{1.5}[Cr^{III}(CN)_6]\cdot nD_2O$ where $x=0$, 0.4 and 1. Fig. 7 shows the MAS D NMR spectrum of these compounds measured at 299 K. The isotropic shift is +65 and −15 ppm for $Mn_{1.5}^{II}[Cr^{III}(CN)_6]\cdot nD_2O$ and $Ni_{1.5}^{II}[Cr^{III}(CN)_6]\cdot nD_2O$, respectively. The spectrum of $(Ni_{0.4}^{II}Mn_{0.6}^{II})_{1.5}[Cr^{III}(CN)_6]\cdot nD_2O$ is not a superposition of the two spectra of $Mn_{1.5}^{II}[Cr^{III}(CN)_6]\cdot nD_2O$ and $Ni_{1.5}^{II}[Cr^{III}(CN)_6]\cdot nD_2O$ but its isotropic shift locates at +35 ppm, just at the weighted average of those of the Mn and Ni salts. These isotropic shifts and their

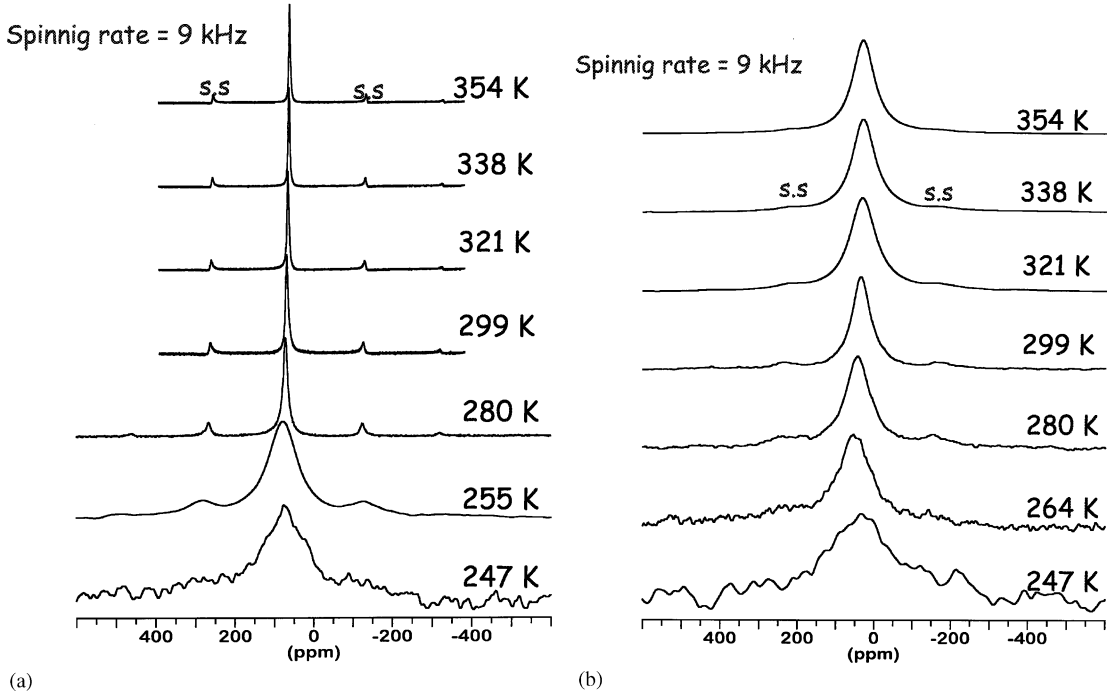

Fig. 8. Temperature variation of the MAS D NMR spectrum of (a) $Mn_{1.5}^{II}[Cr^{III}(CN)_6]\cdot nD_2O$ and (b) $(Ni_{0.4}^{II}Mn_{0.6}^{II})_{1.5}[Cr^{III}(CN)_6]\cdot nD_2O$. Spinning side bands are indicated by an abbreviation s.s.

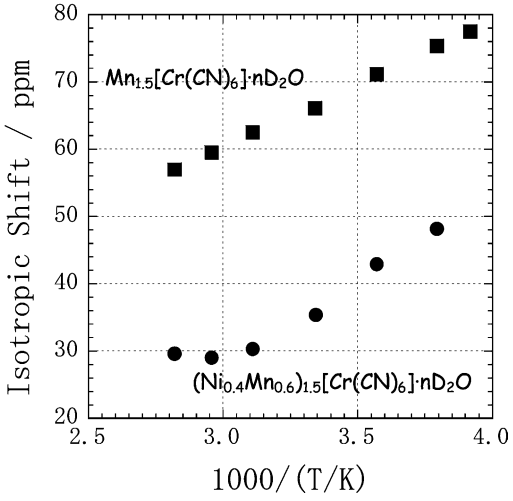

Fig. 9. Temperature dependence of the isotropic shift of the deuterium NMR for $Mn^{II}_{1.5}[Cr^{III}(CN)_6]\cdot nD_2O$ (■) and $(Ni^{II}_{0.4}Mn^{II}_{0.6})_{1.5}$-$[Cr^{III}(CN)_6]\cdot nD_2O$ (●).

temperature dependence depicted in Fig. 8 indicate that the crystal water molecules of the mixed system $(Ni^{II}_{0.4}Mn^{II}_{0.6})_{1.5}[Cr^{III}(CN)_6]\cdot nD_2O$ sense an averaged hyperfine field of Ni and Mn ions and that the crystal water molecules are tightly bound to neither the Ni nor Mn ion down to 250 K at least. The isotropic shift of MAS D NMR spectrum of both $Mn^{II}_{1.5}[Cr^{III}(CN)_6]\cdot nD_2O$ and $(Ni^{II}_{0.4}Mn^{II}_{0.6})_{1.5}[Cr^{III}(CN)_6]\cdot nD_2O$ moves to higher frequency as the temperature is decreased as shown in Fig. 9, indicating that the crystal water molecules sense a positive hyperfine field.

Acknowledgements

This research was supported by The Mitsubishi Foundation and by grant-in-aid for Scientific Research on Priority Areas (A) from the Ministry of Education, Culture, Sports, Science and Technology of Japan.

References

[1] O. Sato, T. Iyoda, A. Fujishima, K. Hashimoto, Science 272 (1996) 704.
[2] A. Bleuzen, C. Lomenech, A. Dolbecq, F. Villain, A. Goujon, O. Roubeau, M. Nogues, F. Varret, F. Baudelet, E. Dartyge, C. Giorgetti, J.J. Gallet, C.C. Dit Moulin, M. Verdaguer, Mol. Cryst. Liq. Cryst. 335 (1999) 253.
[3] S. Ohkoshi, T. Iyoda, A. Fujishima, K. Hashimoto, Phys. Rev. B 56 (1997) 11642.
[4] O. Sato, Y. Einaga, T. Iyoda, A. Fujishima, K. Hashimoto, J. Phys. Chem. 101 (1997) 3903.
[5] T. Kawamoto, Y. Asai, S. Abe, Phys. Rev. B 60 (1999) 12990.
[6] S. Ohkoshi, H. Tokoro, M. Utsunomiya, M. Mizuno, M. Abe, K. Hashimoto, J. Phys. Chem. 106 (2002) 2423.
[7] R. Kurland, B.R. McGervey, J. Magn. Resonance 2 (1970) 286.
[8] J.P. Jesson, in: G.N. La Mar, W.De.W. Horrocks, Jr., R.H. Holm (Eds.), NMR of Paramagnetic Molecules, Academic Press, 1973.
[9] G. Maruta, S. Takeda, R. Imachi, T. Ishida, T. Nogami, K. Yamaguchi, J. Am. Chem. Soc. 121 (1999) 424.
[10] P.A. Beckmann, C. Dybowski, J. Magn. Resonance 146 (2000) 379.
[11] F.V.D. Cruser, E.H. Miller, J. Am. Chem. Soc. 28 (1906) 1132.
[12] H. Tokoro, S. Ohkoshi, K. Hashimoto, private communication.
[13] S. Takeda, Y. Umehara, H. Hara, G. Maruta, Mol. Cryst. Liq. Cryst. 379 (2002) 253.
[14] C.A. Daul, P. Day, F.R.S., B.N. Figgis, H.U. Gudel, F. Herren, A. Ludi, P.A. Reynolds, Proc. R. Soc. Lond. A 419 (1988) 205.